

Pressure-induced charge transfer and dT_c/dP in $YBa_2Cu_3O_{7-x}$

J.D. Jorgensen^a, Shiyou Pei^b, P. Lightfoot^b, D.G. Hinks^a, B.W. Veal^a, B. Dabrowski^b,
A.P. Paulikas^a and R. Kleb^a

^a Materials Science Division and

^b Science and Technology Center for Superconductivity, Argonne National Laboratory, Argonne, IL 60439, USA

I.D. Brown

Institute for Materials Research, McMaster University, Hamilton, Ontario, Canada L8S 4M1

Received 19 July 1990

Subtle pressure-induced structural changes in $YBa_2Cu_3O_{6.93}$ and $YBa_2Cu_3O_{6.60}$ have been measured by neutron powder diffraction for samples in a hydrostatic helium-gas pressure cell. Small, but significant, differences in the compression of particular Cu–O bonds (notably Cu(2)–O(4)) are observed. However, when the charges on the two copper sites are calculated, requiring overall charge conservation versus pressure, it is found that the net pressure-induced charge transfer of holes from Cu(1) to Cu(2) is essentially the same for both systems. We conclude that the much smaller value of dT_c/dP for $YBa_2Cu_3O_{6.93}$ results from the fact that, in the 90 K superconductor, the T_c has already reached its optimum value and the introduction of additional hole carriers cannot further increase T_c .

1. Introduction

The oxide superconductors exhibit a remarkable range for the pressure dependence of the superconducting transition temperature (dT_c/dP) [1,2]. For some compounds dT_c/dP is the largest observed for any superconductors, while for others it is zero or negative. Additionally, for a single compound, dT_c/dP may vary over a wide range as T_c is varied by changing the chemical composition (e.g., by changing the oxygen content). Perhaps the most striking example of this behavior occurs in the $MBa_2Cu_3O_{7-x}$ (1–2–3) system ($M=Y, La, Eu, Er$, etc.) where both T_c and dT_c/dP are functions of the oxygen composition, x . For example, for $EuBa_2Cu_3O_{7-x}$, Chu et al. [3] reported $dT_c/dP=1$ K/GPa for the 90 K superconductor with $x\approx 0-0.1$ and $dT_c/dP=9$ K/GPa for the 60 K superconductor with $x\approx 0.4$. Similar behavior occurs for $YBa_2Cu_3O_{7-x}$ although the reported values for dT_c/dP for oxygen-deficient ($T_c\approx 60$ K) samples vary from 4 to 7 K/GPa [2,4]. The differences may result from the way T_c was measured, since the superconducting transitions are often

observed to broaden under pressure. In all cases for the 1–2–3 superconductor, however, dT_c/dP increases markedly as T_c is decreased by removing oxygen.

Superconductivity in the 1–2–3 compounds is thought to depend on a charge transfer phenomenon. Hole carriers are created in the CuO_2 planes by the transfer of electrons from the planes to the CuO_{1-x} chains [5,6]. T_c is a function of the effective valence of the copper atoms (Cu(2)) in the planes [6]. The amount of charge transfer is controlled by the oxidation state of the copper atoms (Cu(1)) in the chains, which varies with the oxygen content, $7-x$, and the crystal structure. When oxygen content is varied, the dominant effect is to change the oxidation state of Cu(1). The charge transfer to the planes is a minor effect, but a surprisingly small change in the amount of transferred charge gives rise to the variation of T_c from 0 to 90 K. This balance between the oxidation/reduction of Cu(1) and the transfer of charge between Cu(1) and Cu(2) clearly depends in a critical way on the crystal structure.

Thus, one explanation for the large dT_c/dP ob-

served for some oxide superconductors is that pressure modifies the structure in a way that increases the number of hole carriers in the CuO_2 plane through charge transfer. Such a concept appears to explain the behavior of $YBa_2Cu_4O_8$ where an unusually large pressure-induced change in a particular Cu–O bond length has been interpreted as evidence for pressure-induced charge transfer consistent with the large dT_c/dP for that compound [7].

In this paper we report structural studies as a function of pressure for two different oxygen compositions of $YBa_2Cu_3O_{7-x}$; $x=0.7$ with $T_c=90$ K and $x=0.40$ with $T_c=60$ K. Since these compositions are known to exhibit widely different behavior for dT_c/dP , a comparison of the pressure-induced structural changes offers a unique test of the concept of pressure-induced charge transfer as an explanation for the pressure dependence of T_c .

2. High-pressure neutron powder diffraction

Powder samples of $YBa_2Cu_3O_{6.93}$ with $T_c=91$ K and $YBa_2Cu_3O_{6.60}$ with $T_c=58$ K were synthesized and characterized as described in previous publications [5,8]. Time-of-flight neutron powder diffraction data were collected on the Special Environment Powder Diffractometer [9] at Argonne's Intense Pulsed Neutron Source (IPNS) with the samples in a helium-gas pressure cell. The helium-gas pressure cell offers the advantages of perfectly hydrostatic conditions, precise pressure measurement, and (owing to the fixed-angle, time-of-flight technique) diffraction data that are completely free from Bragg scattering from the cell. The maximum pressure is limited to about 0.65 GPa.

Although this pressure cell has been used for previous measurements at IPNS [10–12], its unique design features have never been described in detail. The time-of-flight neutron diffraction technique offers significant advantages for studies in high-pressure cells because of the ability to collect the entire data set at a fixed scattering angle [13]. Since, in high-pressure studies of powder samples, the sample must be supported by the wall of the vessel (unlike the situation for furnaces and low-temperature environments), avoiding scattering from the pressure cell while maximizing the effective volume of sam-

ple illuminated by the incident neutron beam and seen by the detectors is difficult. In the time-of-flight design used here, a scattering angle of $2\theta=90^\circ$ is chosen to allow the best possible collimation.

An exploded view of the pressure cell is shown in fig. 1. The cell is similar to others that have been used for neutron diffraction [14,15] except for the incorporation of internal gadolinium-epoxy shielding. The cell is constructed from three concentric cylinders of 7075-T6 alloy aluminum. The gadolinium-epoxy shielding is cast into depressions approximately 0.25 mm deep milled into the surfaces of the inner two cylinders. After the epoxy hardens, these cylinders are machined to the final size and the cell is assembled. The inner bore (1.27 cm in diameter) is then autofrettaged to the final size by pressurizing the cell with oil to 0.7 GPa. The seal is a mechanically preloaded Bridgman unsupported-area seal with gaskets of lead, indium, teflon, and neoprene.

The gadolinium-epoxy shielding serves two functions. The first is to collimate the incident and scattered neutron beams at a point as close as possible to the sample. In the present design, the shielding defines incident and scattered beams 0.64 cm wide. The second purpose is to minimize backgrounds that result from multiple scattering of neutrons in the aluminum. Multiply scattered neutrons possess no correlation between wavelength and direction, and thus contribute to a featureless background in a time-of-flight experiment. These neutrons will be seen by the detectors if the first scattering process occurs in a region of the aluminum cell illuminated by the incident (straight-through) beam and the final scattering process occurs in a region of the aluminum seen by the detectors. The internal gadolinium-epoxy shielding eliminates many such paths and results in a significant reduction in the background. Additional cadmium shielding on the outer surface of the cell (not shown in fig. 1) is used to mask all of the cell surface except the window regions and serves the same two functions.

The sample is installed in the pressure cell by first containing it in a 1.14 cm OD thin-walled vanadium can. The helium gas flows through small filters constructed by packing steel wool into holes in the aluminum end caps of the can. This method of enclosing the sample ensures that particles of the sample powder do not plug the helium capillary line. The

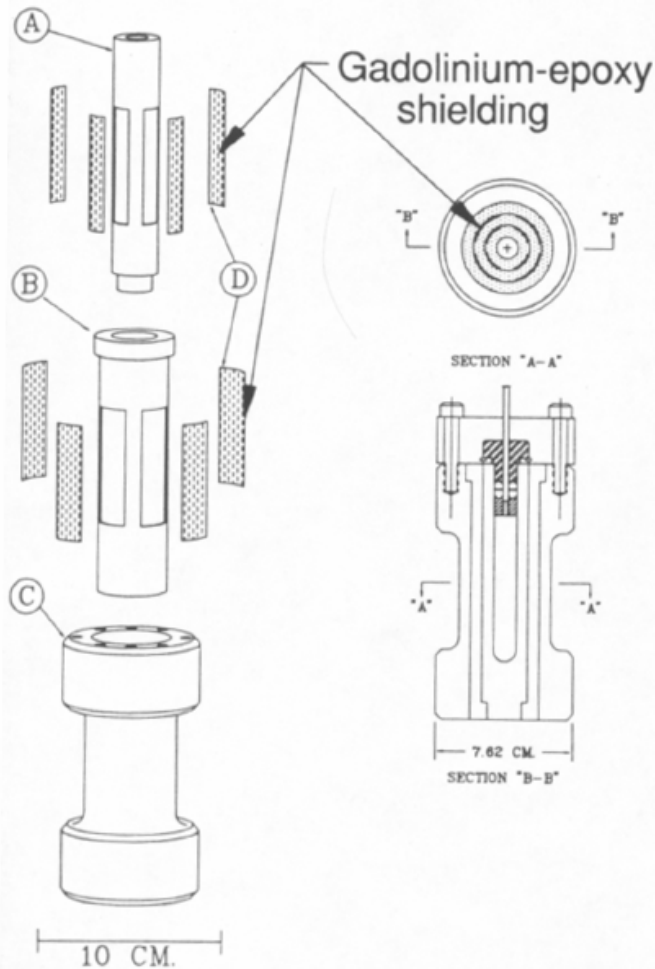


Fig. 1. Exploded view of the helium-gas pressure cell used for time-of-flight neutron powder diffraction. The cell is constructed from three concentric cylinders of 7075-T6 alloy aluminum. Windows for the incident, transmitted ($2\theta=0^\circ$), and scattered ($2\theta=90^\circ$) neutron beams are formed by collimating with internal gadolinium-epoxy shielding.

pressure cell accommodates a sample can 1.14 cm in diameter and 6.4 cm long. The active sample volume illuminated by neutrons is 4.8 cm long.

3. Results and discussion

For each sample, data were collected at seven pressures up to a maximum pressure of about 0.58 GPa. Data were collected for about 3 hours at each pressure. The data were analyzed by the Rietveld technique [16] to give lattice parameters, atom positions, and isotropic temperature factors at each pressure. The Rietveld refinements included ap-

proximately 350 Bragg reflections over the range of d spacings from 0.71 Å to 3.90 Å. Figure 2 shows the Rietveld refinement profile for $YBa_2Cu_3O_{6.93}$ at 0.58 GPa. All of the refinements were of similar quality. The refined parameters for both compositions are listed in table I.

The unit cell compressions for the two samples are amazingly similar. Lattice parameters and cell volumes versus pressure are compared in fig. 3. The behavior is virtually identical along the a - and c -axes. Along the b -axis, $YBa_2Cu_3O_{6.60}$ exhibits a slightly larger compression than $YBa_2Cu_3O_{6.93}$. This may result directly from the partial occupancy of the CuO_{1-x} chains along the b -axis in the $YBa_2Cu_3O_{6.60}$ sample, making the structure somewhat more compressible along the chain direction.

The average compressibilities along the three crystallographic axes and the volume compressibilities and bulk moduli, based on least-squares fits of straight lines to the data, are given in table II. The compression is approximately a factor of two larger along the c -axis than in the basal plane. This anisotropic compressibility is to be expected for an anisotropic structure such as that of $YBa_2Cu_3O_{7-x}$. The largest compression is along the c -axis due to the comparatively weak bonding along that direction.

The compression of $YBa_2Cu_3O_{7-x}$ has also been measured in several X-ray diffraction studies [1,17-22]. Reported values for the bulk modulus, B , range between 100 and 196 GPa for the 90 K superconducting composition. Only a few authors attempted to report linear compressibilities along the a -, b - and c -axes. Moreover, as pointed out by Fietz et al. [21], the nearly pseudocubic cell constants sometimes led to confusion in indexing the high-pressure X-ray diffraction patterns and the anisotropy in compression was interpreted incorrectly in some of the earlier work. Our value for the bulk modulus of the 90 K compound falls in the lower range of the (widely spread) previously reported values and agrees very well with the recent analysis of Ledbetter and Lei [23] who discuss the large discrepancies based on the X-ray data and calculate the bulk modulus from other measured and calculated physical properties.

We would propose two possible explanations for the large variation among the various high-pressure diffraction measurements. To begin with, the compressibilities are pressure dependent, generally de-

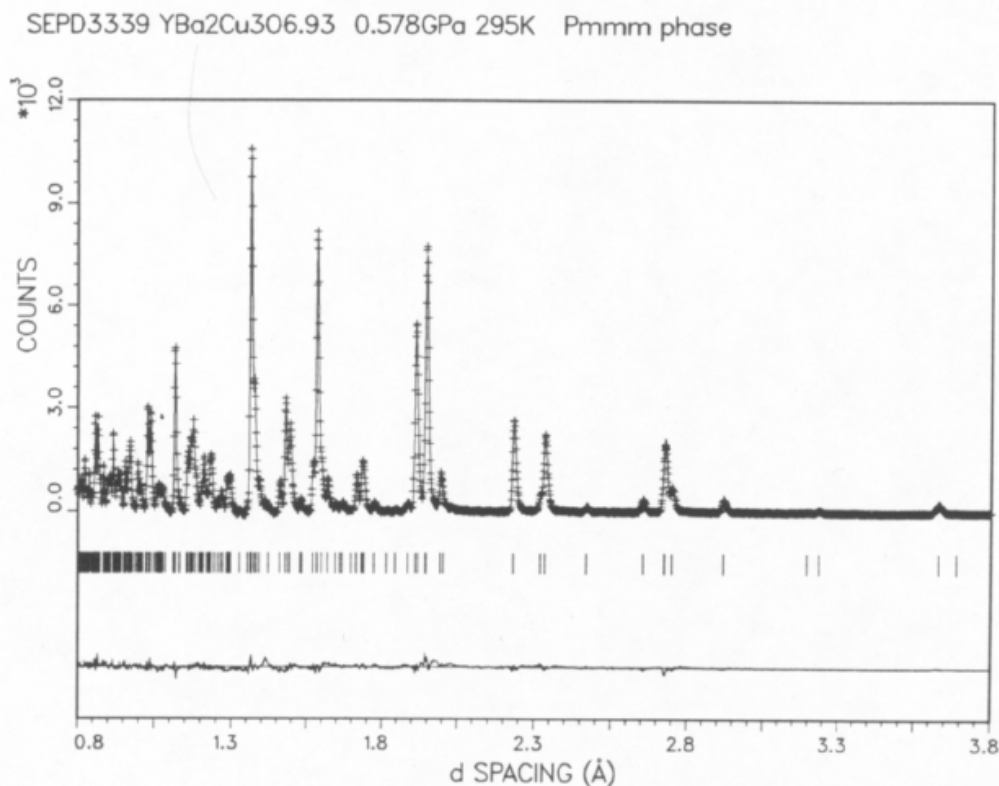


Fig. 2. Rietveld refinement profile for $\text{YBa}_2\text{Cu}_3\text{O}_{6.93}$ at 0.58 GPa. Plus signs (+) are the raw time-of-flight neutron powder diffraction data. The solid line is the calculated profile. Tick marks below the profile mark the positions of allowed Bragg reflections. The background was fit as part of the refinement but has been subtracted prior to plotting. A difference curve (observed minus calculated) is plotted at the bottom.

creasing with increasing pressure. Thus, our work, which is based on a high-precision measurement at comparatively low pressures, will tend to give a higher compressibility. This effect alone, however, probably does not account for the differences. Additional errors probably arise from nonhydrostatic conditions for some of the previous measurements. If the pressure is nonhydrostatic, both the volume compressibility and (especially) the anisotropy of compression will be incorrectly measured.

It is well known that compression can give rise to changes in electronic structure. Such changes can be substantially larger when the compression is anisotropic. This can be understood in either of two equivalent ways. In a band picture, anisotropic compression moves bands with respect to one another, with the Fermi energy also moving to conserve charge. It is well known that pressure induced electronic transition occurs in this way in compounds with anisotropic compressibilities [24]. In a charge-transfer picture, anisotropic compression

can change the coordination spheres of the two inequivalent copper atoms in different ways. Since total charge is conserved, charge redistribution may occur.

If anisotropic compression results in changes in the electronic structure of $\text{YBa}_2\text{Cu}_3\text{O}_{7-x}$, changes in the effective valences of the atoms should be present. It has already been shown that particular Cu–O bond lengths, especially the bonds to the apical oxygen atom O(4), are sensitive probes of the charge distribution in this system [5,6,18]. The Cu(1)–O(4) and Cu(2)–O(4) bond lengths versus pressure are plotted in fig. 4. The behavior of Cu(1)–O(4) is nearly identical for the two oxygen compositions, but the pressure-induced change in Cu(2)–O(4) is significantly larger for $\text{YBa}_2\text{Cu}_3\text{O}_{6.60}$. This difference is more easily seen by plotting the fractional change in Cu(2)–O(4) $[\Delta(\text{Cu}(2)\text{--O}(4))/(\text{Cu}(2)\text{--O}(4))_{p=0}]$ as shown in fig. 5. The pressure-induced change for $\text{YBa}_2\text{Cu}_3\text{O}_{6.60}$ is a factor of two larger than that for $\text{YBa}_2\text{Cu}_3\text{O}_{6.93}$. Additionally, the change of

Table I

Structural parameters versus pressure for $YBa_2Cu_3O_{6.93}$ and $YBa_2Cu_3O_{6.60}$. The oxygen occupancies are fixed at their stoichiometric values for O(2), O(3) and O(4), and at the average refined values (for all pressures) for O(1) and O(5).

$YBa_2Cu_3O_{6.93}$: $n(O(1))=0.89$; $n(O(2))=n(O(3))=n(O(4))=2$; $n(O(5))=0.00$							
	P (GPa)						
	0.000	0.102	0.207	0.310	0.416	0.496	0.578
a (Å)	3.8182(1)	3.8172(1)	3.8162(1)	3.8154(1)	3.8145(1)	3.8138(1)	3.8133(1)
b (Å)	3.8841(1)	3.8833(1)	3.8827(1)	3.8820(1)	3.8813(1)	3.8808(1)	3.8804(1)
c (Å)	11.6831(3)	11.6780(3)	11.6732(3)	11.6674(3)	11.6626(3)	11.6585(3)	11.6542(3)
V (Å ³)	173.259	173.103	172.959	172.806	172.663	172.549	172.445
z : Ba	0.1822(3)	0.1824(4)	0.1827(4)	0.1826(4)	0.1829(4)	0.1829(4)	0.1828(4)
z : Cu(2)	0.3544(2)	0.3544(2)	0.3545(2)	0.3544(2)	0.3544(4)	0.3545(2)	0.3548(2)
z : O(2)	0.3745(4)	0.3746(4)	0.3745(3)	0.3747(4)	0.3746(3)	0.3748(3)	0.3749(3)
z : O(3)	0.3762(3)	0.3764(4)	0.3764(4)	0.3765(4)	0.3767(4)	0.3766(4)	0.3765(4)
z : O(4)	0.1609(3)	0.1610(3)	0.1607(3)	0.1610(3)	0.1610(3)	0.1611(3)	0.1613(3)
R_{wp} (%)	10.76	11.13	10.41	10.65	10.03	10.04	9.88
R_{exp} (%)	3.00	5.12	4.43	4.93	4.53	4.62	4.34

$YBa_2Cu_3O_{6.60}$: $n(O(1))=0.63$; $n(O(2))=n(O(3))=n(O(4))=2$; $n(O(5))=0.01$							
	P (GPa)						
	0.000	0.103	0.208	0.310	0.415	0.489	0.563
a (Å)	3.8300(1)	3.8290(1)	3.8280(1)	3.8271(1)	3.8261(1)	3.8255(1)	3.8248(1)
b (Å)	3.8850(1)	3.8840(1)	3.8833(1)	3.8822(1)	3.8816(1)	3.8808(1)	3.8803(1)
c (Å)	11.7087(3)	11.7025(3)	11.6973(3)	11.6912(3)	11.6867(3)	11.6831(3)	11.6797(3)
V (Å ³)	174.217	174.034	173.880	173.700	173.560	173.443	173.339
z : Ba	0.1878(3)	0.1874(3)	0.1875(2)	0.1873(3)	0.1874(2)	0.1873(2)	0.1872(3)
z : Cu2	0.3569(2)	0.3570(2)	0.3568(2)	0.3569(2)	0.3569(2)	0.3567(2)	0.3567(2)
z : O2	0.3766(3)	0.3766(3)	0.3763(3)	0.3762(3)	0.3764(3)	0.3762(3)	0.3764(3)
z : O3	0.3787(3)	0.3785(3)	0.3788(3)	0.3790(3)	0.3786(3)	0.3787(3)	0.3784(3)
z : O4	0.1578(2)	0.1578(2)	0.1578(2)	0.1579(2)	0.1579(2)	0.1581(2)	0.1581(2)
R_{wp} (%)	8.98	8.11	7.94	8.02	7.92	8.06	7.88
R_{exp} (%)	4.82	4.18	4.34	4.53	4.38	4.64	4.40

the Cu(2)–O(4) bond length for $YBa_2Cu_3O_{6.60}$ is a factor of two larger than the average compression along the c -axis, while that for $YBa_2Cu_3O_{6.93}$ is comparable to its c -axis compression. Thus, the compression of this bond is markedly enhanced for the $YBa_2Cu_3O_{6.60}$ composition, while it simply follows the unit cell compression along the same direction for $YBa_2Cu_3O_{6.93}$. Similar behavior has recently been observed in $La_{1.85}Sr_{0.15}CuO_4$, where high-pressure neutron powder diffraction measurements show that the apical Cu–O bond length compresses at a rate essentially twice that of the c -axis compression [25].

The process can be understood in simple physical terms. The application of pressure along the c -axis will bring Cu(1) and Cu(2) closer together. In ad-

dition to the normal bond compressibility, the stress can be relieved by charge transfer. Ignoring the overall compression resulting from the application of pressure, charge conservation dictates that as one of the Cu–O(4) bonds is compressed the other must elongate, a net reduction in the Cu(1)–Cu(2) distance is achieved by compressing the softer bond (Cu(2)–O(4) and elongating the stiffer bond (Cu(1)–O(4)), resulting in a transfer of charge from Cu(1) to Cu(2). The observed changes in bond lengths are in agreement with these concepts (after normalizing for the effects of overall compression along the c -axis), even though the size of the changes is comparable to the experimental uncertainty.

Taken at face value, the difference in pressure-in-

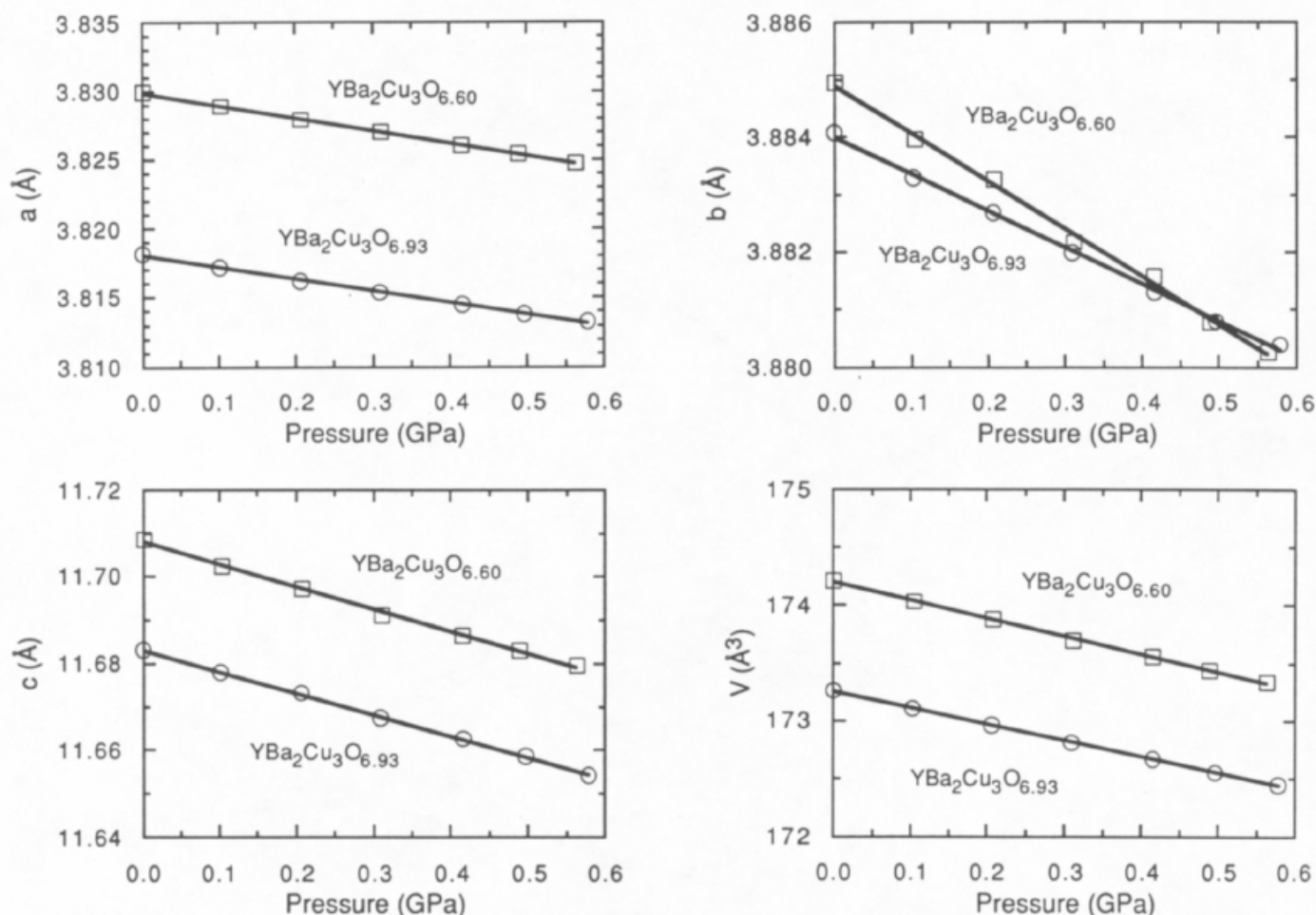


Fig. 3. Lattice parameters a , b , and c , and unit cell volume V versus pressure for $\text{YBa}_2\text{Cu}_3\text{O}_{6.93}$ and $\text{YBa}_2\text{Cu}_3\text{O}_{6.60}$. Error bars are smaller than the symbols.

Table II

Linear and volume compressibilities and bulk modulus, B , for $\text{YBa}_2\text{Cu}_3\text{O}_{6.93}$ and $\text{YBa}_2\text{Cu}_3\text{O}_{6.60}$ based on a least-squares fit of a straight line to the parameters refined from neutron powder diffraction data.

	$\text{YBa}_2\text{Cu}_3\text{O}_{6.93}$	$\text{YBa}_2\text{Cu}_3\text{O}_{6.60}$
$(da/dP)/a_0$ (GPa^{-1})	-2.22×10^{-3}	-2.40×10^{-3}
$(db/dP)/b_0$ (GPa^{-1})	-1.65×10^{-3}	-2.14×10^{-3}
$(dc/dP)/c_0$ (GPa^{-1})	-4.26×10^{-3}	-4.39×10^{-3}
$(dV/dP)/V_0$ (GPa^{-1})	-8.12×10^{-3}	-8.92×10^{-3}
B (GPa)	123	112

duced bond compression of the $\text{Cu}(2)\text{--O}(4)$ bond for the two compositions might be interpreted as evidence for a larger charge transfer in the $\text{YBa}_2\text{Cu}_3\text{O}_{6.60}$ compound. However, a proper calculation of the charges on $\text{Cu}(1)$ and $\text{Cu}(2)$, based on bond valences [26], where the sum of charges on $\text{Cu}(1)$ and $\text{Cu}(2)$ is conserved as a function of pressure, shows

that the pressure-induced charge transfer is nearly identical in the two compounds.

The bond valence sum formalism has been demonstrated to provide useful information about the distribution of charges in $\text{YBa}_2\text{Cu}_3\text{O}_{7-x}$ [26]. For example, in the case of oxygen-deficient $\text{YBa}_2\text{Cu}_3\text{O}_{7-x}$, a striking correlation between the ef-

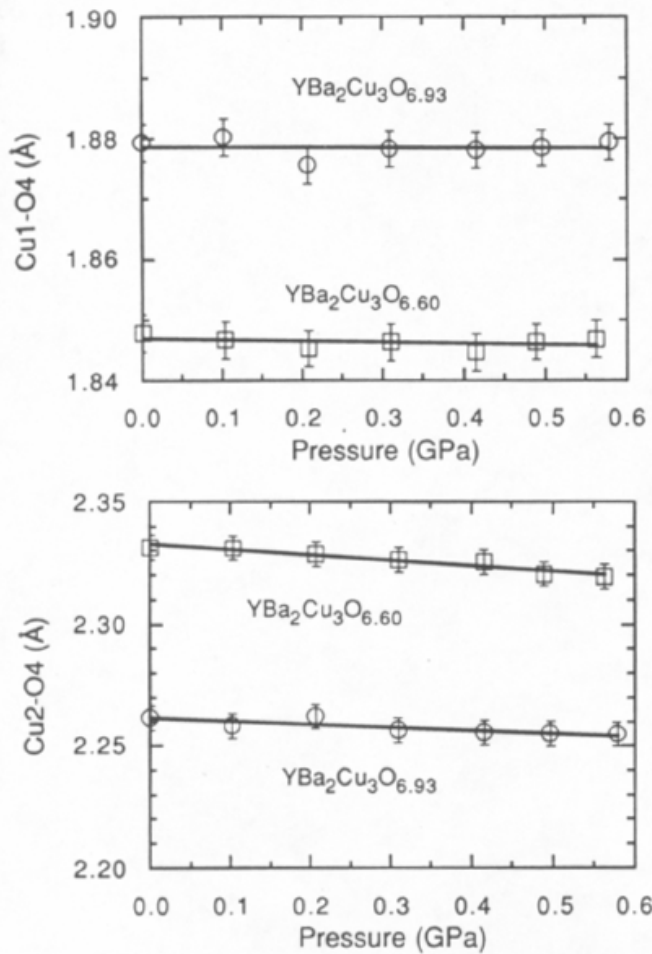


Fig. 4. Cu(1)-O(4) and Cu(2)-O(4) bonds lengths versus pressure for $YBa_2Cu_3O_{6.93}$ and $YBa_2Cu_3O_{6.60}$.

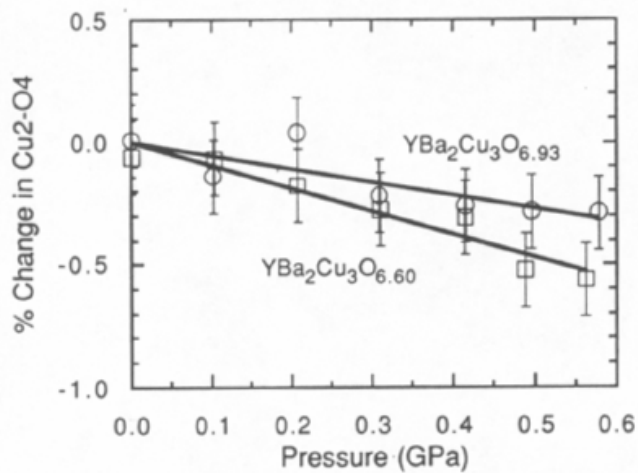


Fig. 5. Comparison of the fractional changes in Cu(2)-O(4) bond lengths (expressed as a percentage) versus pressure for $YBa_2Cu_3O_{6.93}$ and $YBa_2Cu_3O_{6.60}$.

fective charge on Cu(2) and T_c has been observed [6]. However, the application of these techniques to high-pressure data is not straightforward and has not previously been attempted. For interpreting high-pressure data, it must be realized that the coefficients, r_0 and B , normally taken as constants in the bond valence sum equation

$$S_i = \sum_j e^{(r_0 - r_{ij})/B}, \quad (1)$$

are actually pressure dependent. The pressure dependence is not known, a priori. However, we have taken the approach that the correct behavior can be learned by requiring overall charge conservation in the structure. For the present calculations, we have assumed that the valences of Cu(1) and Cu(2) are the only ones that are variable. Since the same value of B has been shown to work for essentially all atoms [27], we have assumed that the pressure dependence of B can be neglected. (Moreover, since the overall effect is small, the correct behavior can be adequately approximated by assigning all of the pressure dependence to one variable.)

The pressure dependence of r_0 for each of the sample compositions can be obtained by requiring that the weighted sum of charges on Cu(1) and Cu(2) [i.e., $S(\text{Cu}(1)) + 2S(\text{Cu}(2))$] be a constant. This calculation yields the changes in r_0 versus pressure shown in fig. 6. The pressure dependence is somewhat different for the two compositions, but, since we are interested in evaluating small changes in the

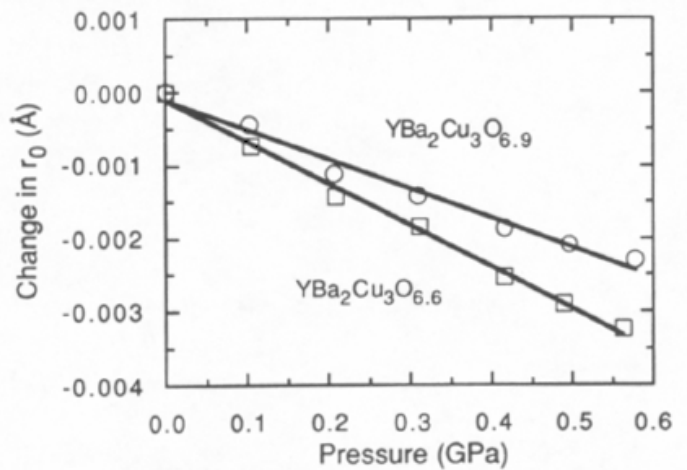


Fig. 6. Changes in the coefficient r_0 in the bond valence sum [eq. (1)] versus pressure obtained by requiring conservation of charge between Cu(1) and Cu(2).

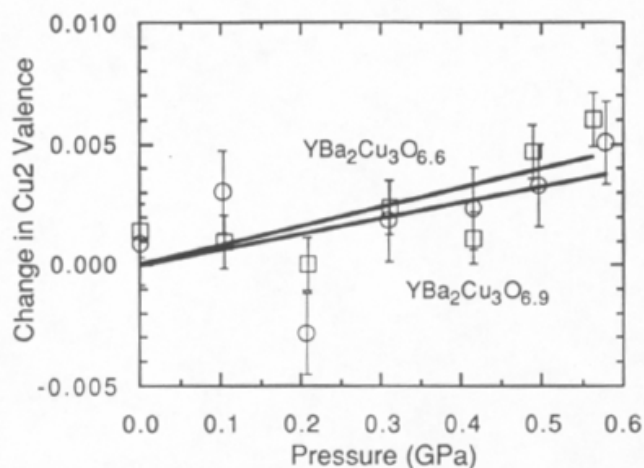


Fig. 7. Change in the charge on Cu(2) versus pressure obtained from the values of r_0 defined by the linear least-squares fits of fig. 6 and the refined structural parameters in table I.

bond valence sums, not absolute values, these differences are probably not serious. The solid lines in fig. 6 are linear least-squares fits to the data and are used in subsequent calculations as the best values for $r_0(P)$.

Having established the pressure dependence of r_0 required to give charge conservation, we use these values to calculate the bond valence sums for Cu(1) and Cu(2) versus pressure. For both compositions, additional holes are transferred to the Cu(2)-O planes with increasing pressure. However, the rate of charge transfer is essentially identical; $dQ/dP = 0.0065$ holes/GPa for $YBa_2Cu_3O_{6.93}$ and 0.0080 holes/GPa for $YBa_2Cu_3O_{6.60}$. This is most clearly shown in fig. 7, where the changes in Cu(2) valence versus pressure are plotted.

We have tried several alternative methods for calculating the pressure-induced charge transfer. For example, the explicit pressure dependence of r_0 can be ignored in the initial calculation of bond valence sums. Charge conservation is then invoked by requiring that the weighted sum of charges on Cu(1) and Cu(2) be constant. The amount of charge transfer is, thus, the appropriate average of the changes for Cu(1) and Cu(2). Such a calculation yields a result essentially identical to that given above. Our conclusion, after exploring several such methods of calculation are that they are (to first order) equivalent. Using any model that assumes that Cu(1) and Cu(2) are the only atoms that can exhibit changes in valence, and requiring charge conservation as a

function of pressure, leads to the same conclusion, namely that the pressure-induced charge transfer in the two compositions is essentially the same.

The expected rate of change of T_c with hole concentration, dT_c/dQ , can be estimated from previous measurements on $YBa_2Cu_3O_{7-x}$ versus x [6] and chemically-substituted $YBa_2Cu_3O_{7-x}$ [27]. In the first case, the valence of Cu(2) was calculated directly from the Cu(2) bond valence sum [6]. Since the total charge in the system varies with the changing oxygen content, the total charge was not normalized as has been done in the present case. Such an approach may be subject to some error because it ignores the effects of competing internal strains [26]. Averaged over the range of oxygen concentrations that give $0 \leq T_c \leq 0$ K, such a calculation yields $dT_c/dQ \approx 1100$ K/e. In the second case [28], the average copper valence for the compound was determined by chemical titration. This valence was then partitioned between Cu(1) and Cu(2) based on self-consistency arguments. Using this approach, an approximate value of $dT_c/dQ \approx 500$ K/e was obtained.

The latter experiment [28] illustrated another feature of the relationship between charge transfer and T_c , namely that T_c is not a linear function of the number of holes in the CuO_2 planes. Rather, T_c increases sharply with the number of holes for hole concentrations less than 0.2, but appears to approach a limiting maximum value for higher hole concentrations. Similar behavior was even more clearly observed in later studies of $La_{2-x}Sr_xCuO_4$ versus x [29]. Here, there appears to be an optimum hole concentration near 0.2 where T_c reaches its maximum value. Beyond that concentration, T_c actually drops with increasing hole concentration.

The pressure-induced changes in T_c and charge transfer in $YBa_2Cu_3O_{7-x}$ can be readily understood in terms of these principles. In the case of $YBa_2Cu_3O_{6.60}$, the observed charge transfer, 0.0080 holes/GPa, corresponds to a predicted change in T_c of $4-9$ K/GPa, in good agreement with the measured values of $4-7$ K/GPa [2,4]. For $YBa_2Cu_3O_{6.93}$, which has a higher initial hole concentration, we would conclude that, even though nearly the same amount of charge transfer occurs, the increase in T_c is much smaller because the optimum hole concentration has already been reached. Such a conclusion is supported by the observation that applied pressure

does not indefinitely increase the T_c of oxygen-deficient $60\text{ K } YBa_2Cu_3O_{7-x}$ [3]. Rather, above 10 GPa the T_c appears to plateau in the region of 90 K.

4. Conclusions

We conclude that the anisotropic structure of $YBa_2Cu_3O_{7-x}$ gives rise to anisotropic compression and, consequently, pressure-induced charge transfer between the Cu(1) and Cu(2) planes. Based on our present attempts to apply bond valence sum methods to the high-pressure data, we conclude, however, that the amount of charge transfer is essentially the same for the compositions $YBa_2Cu_3O_{6.93}$ and $YBa_2Cu_3O_{6.60}$. Thus, the large difference in dT_c/dP reported for these compositions cannot be explained in terms of a large difference in the amount of pressure-induced charge transfer. Rather, we conclude that the oxygen-deficient $YBa_2Cu_3O_{6.60}$ compound, whose initial T_c is 60 K, exhibits the expected behavior, while the fully oxygenated $YBa_2Cu_3O_{6.93}$ compound, whose initial T_c is 90 K, shows no pressure-induced variation of T_c because the T_c has already "saturated" at its optimum value; i.e., an increase in the number of holes in the CuO_2 plane does occur, but does not lead to an increase in T_c . An extension of these ideas may explain the unusually large variation in dT_c/dP for other oxide superconductors.

Acknowledgements

This work is supported by the US Department of Energy, Division of Basic Energy Sciences, Office of Materials Sciences, under contract No. W-31-109-ENG-38 (JDJ, DGH, BWV, APP and RK), the National Science Foundation, Science and Technology Center for Superconductivity, under grant No. DMR 88-09854 (SP and PL), and the Natural Science and Engineering Research Council of Canada (IDB).

References

- [1] R.J. Wijngaarden and R.P. Griessen, in: *Studies on High Temperature Superconductors*, Vol. 4, ed. A.V. Narlikar (Nova Science Publishers Inc., New York, 1990) pp. 29–77.
- [2] C. Murayama, N. Mori, S. Yomo, H. Takagi, S. Uchida and Y. Tokura, *Nature* 339 (1989) 293.
- [3] C.W. Chu, Z.J. Huang, R.L. Meng, L. Gao and P.H. Hor, *Phys. Rev. B* 37 (1988) 9730; *Bull. Amer. Phys. Soc.* 33 (1988) 688.
- [4] J.E. Schirber, D.S. Ginley, E.L. Venturini and B. Morosin, *Phys. Rev. B* 35 (1987) 8709; J.G. Huber, W.J. Liverman, Y. Xu and A.R. Moodenbaugh, *Phys. Rev. B* 41 (1990) 8757; J.J. Neumeier, M.B. Maple and M.S. Torikachvili, *Physica C* 156 (1988) 574.
- [5] J.D. Jorgensen, B.W. Veal, A.P. Paulikas, L.J. Nowicki, G.W. Crabtree, H. Claus and W.K. Kwok, *Phys. Rev. B* 41 (1990) 1863.
- [6] R.J. Cava, A.W. Hewat, E.A. Hewat, B. Batlogg, M. Marezio, K.M. Rabe, J.J. Krajewski, W.F. Peck Jr. and L.W. Rupp Jr., *Physica C* 165 (1990) 419.
- [7] E. Kaldis, P. Fischer, A.W. Hewat, E.A. Hewat, J. Karpinski and S. Rusiecki, *Physica C* 159 (1989) 668.
- [8] J.D. Jorgensen, M.A. Beno, D.G. Hinks, L. Soderholm, K.J. Volin, R.L. Hitterman, J.D. Grace, I.K. Schuller, C.U. Segre, K. Zhang and M.S. Kleefisch, *Phys. Rev. B* 36 (1987) 3608.
- [9] J.D. Jorgensen, J. Faber Jr., J.M. Carpenter, R.K. Crawford, J.R. Haumann, R.L. Hitterman, R. Kleb, G.E. Ostrowski, F.J. Rotella and T.G. Worlton, *J. Appl. Crystallogr.* 22 (1989) 321.
- [10] T.G. Worlton, D.L. Decker, J.D. Jorgensen and R. Kleb, *Physica B* 136 (1986) 503.
- [11] A.C. Lawson, R.B. Roof, J.D. Jorgensen, B. Morosin and J.E. Schirber, *Acta Crystallogr. B* 45 (1989) 212.
- [12] H.G. Smith, R. Berliner, J.D. Jorgensen, M. Nielsen and J. Trivisonno, *Phys. Rev. B* 41 (1990) 1231.
- [13] J.D. Jorgensen, in: *Chemical Crystallography with Pulsed Neutrons and Synchrotron X-rays*, eds. M.A. Carrondo and G.A. Jeffrey, NATO ASI Series C: Mathematical and Physical Sciences Vol. 221 (D. Reidel Publishing Co., Dordrecht, 1988) p. 159.
- [14] C.J. Carlile and D.C. Salter, *High Temp.-High Pressures* 10 (1978) 1.
- [15] J. Paureau and C. Vettier, *Rev. Sci. Instrum.* 46 (1975) 1484.
- [16] R.B. VonDreele, J.D. Jorgensen and C.G. Windsor, *J. Appl. Crystallogr.* 15 (1982) 581.
- [17] H. Takahashi, C. Murayama, S. Yomo, N. Mori, W. Ustumi and T. Yagi, *Jpn. J. Appl. Phys.* 26 (Suppl. 26-3) (1987) 1109.
- [18] M.R. Dietrich, W.H. Fietz, J. Ecke and C. Politis, *Jp. J. Appl. Phys.* 26 (Suppl. 26-3) (1987) 1113.
- [19] N.V. Jaya, S. Natarajan and G.V.S. Rao, *Solid State Commun.* 67 (1988) 51.
- [20] J.S. Olsen, S. Steenstrup, I. Johannsen and L. Gerward, *Z. Phys. B - Condensed Matter* 72 (1988) 165.
- [21] W.H. Fietz, M.R. Dietrich and J. Ecke, *Z. Phys. B - Condensed Matter* 69 (1987) 17.
- [22] S. Block, G.J. Piermarini, R.G. Munro and W. Wong-Ng, *Adv. Ceram. Mater.* 2, Special Issue 3B (1987) 601.

- [23] H. Ledbetter and M. Lei, *J. Mater. Res.* 5 (1990) 241.
- [24] J.D. Jorgensen and J.B. Clark, *Phys. Rev. B* 22 (1980) 6149.
- [25] S. Pei, J.D. Jorgensen, D.G. Hinks, B. Dabrowski, P. Lightfoot and D.R. Richards, *Physica C*, in press.
- [26] I.D. Brown, *J. Solid State Chem.* 82 (1989) 122.
- [27] D. Altermatt and I.D. Brown, *Acta Crystallogr. B* 41 (1985) 240;
I.D. Brown, *Acta Crystallogr. B* 44 (1988) 545.
- [28] Y. Tokura, J.B. Torrance, T.C. Huang and A.I. Nazzal, *Phys. Rev. B* 38 (1988) 7156.
- [29] J.B. Torrance, Y. Tokura, A.I. Nazzal, A. Bezing, T.C. Huang and S.S.P. Parkin, *Phys. Rev. Lett.* 61 (1988) 1127;
J.B. Torrance, A. Bezing, A.I. Nazzal, T.C. Huang, S.S.P. Parkin, D.T. Keane, S.J. LaPlaca, P.M. Horn and G.A. Held, *Phys. Rev. B* 40 (1989) 8872;
J.B. Torrance, A. Beizing, A.I. Nazzal and S.S.P. Parkin, *Physica C* 162-164 (1989) 291.